

Continuous melting of a driven two-dimensional vortex lattice with strong pins

L. Fruchter

Laboratoire de Physique des Solides, Bâtiment 510,
Université Paris-Sud, CNRS, 91405 Orsay, France

(Dated: February 7, 2020)

The phase diagram of a driven two-dimensional vortex lattice in the presence of dense quasi-point pins is investigated. The transition from the crystal to the liquid is found continuous at intermediate inductions. The correlations in the pseudo random force that allow for an incomplete unbinding of the dislocations is proposed as a key mechanism to account for the continuous transition.

PACS numbers: 74.25.Dw, 74.60.Ec, 74.72.Bk, 74.72.Yg

I. INTRODUCTION

It has long been noticed that a driven elastic lattice driven at zero temperature may experience pinning as an effective shaking temperature, due to randomly induced displacements of the lattice nodes. This powerful analogy allows for the prediction of some properties of the driven lattice from the common phase diagram of particles with a repulsive interaction. In particular, a dynamical melting transition is predicted and observed numerically [1]. However, strongly disordered systems, as obtained in the presence of strong pins, may move aside from this picture. Indeed, the thermal analogy may break down for the moving crystal due to temporal correlations of the pseudo thermal Langevin force, a situation which is encountered in the case of heterogeneous pinning involving plastic flow channels. As a consequence, while this analogy accounts for the existence of a first order-like dynamical transition, the driven phases may differ from their thermal dynamical analogues. Several examples of such exotic phases have been given in refs. [6, 7, 8]. The anisotropy of the pinning potential, once tilted by the external force, is essential to the formation of these phases [2, 3]. Here, the dynamical transition is examined in detail for a simple system of dense quasi-point pins with positional disorder. For part of the phase diagram, it is found that there is a continuous transition between the crystal and the liquid, through what might be called a liquid crystal, whereas the transition is first order like for the rest of the phase diagram. In the case of the continuous transition, disclinations tend to form chains, which likely arise from the correlations of the pseudo random force which are specific to the driven lattice.

II. EXPERIMENT

The numerical sample used here is the one in ref. [5]. It is the one of two dimensional particles with a repulsive interaction, interacting also with a random attractive potential. The sample mimics a two dimensional vortex lattice, or a three dimensional rigid vortex lattice, in the presence of strong pins, as can be created by heavy ions irradiation. Adopting the terminology of superconduc-

tors, the vortex density is set by the magnetic induction, B , as $n = a_0^{-2} = B = B_0 - B_0$ being the flux quantum carried by each vortex. The repulsive force between vortices is taken as :

$$f_{vv}(r) = (A_v =) K_1(r =) \quad (1)$$

where K_1 is a Bessel function, behaving as $\ln r^{-1}$ at short distance and $r^{-1/2} \exp(-r)$ at large distance. To keep computation tractable, the repulsive force is cut smoothly at a distance $11a_0$, which insures that each particle interacts with many of its closest neighbors.

The short range potential originates from strong pins randomly distributed in the sample, each creating the attractive force:

$$f_p(r) = (2 A_p = r_p) (r = r_p); \text{ for } r = r_p; 0 \text{ for } r > r_p \quad (2)$$

All pins are identical and the randomness of the potential originates from the pins position only.

In the rest, driving current densities are normalized to the single vortex critical current density, $J_c = 2 A_p = r_p B_0$. The density of the pinning sites, relative to that of the vortices, $B_p = B$, is constant and equal to 12. The pinning potential range, relative to the vortex average separation, is also constant and equal to $r_p = a_0 = 5.5 \cdot 10^{-2}$, as well as the reduced force magnitude, $A_p = r_p A_v = 20$. As a consequence, using a_0 as the length scale, the different numerical experiments made for different values of the induction B only differ by the reduced vortex interaction length, $=a_0$. As in [5], the total force on each vortex, originating from its neighbors, a possible pinning site at the vortex location and the uniform external force is computed at each time step. Vortices are then moved on a time interval small enough so that their motion is small compared to all characteristic lengths. The boundary conditions are cyclic along the driving force direction. A large area free from any pinning site is kept at the sample edges, where a perfect hexagonal lattice is obtained under the action of the external magnetic pressure. All measurement are made far from the sample edges, in the pinned region, where the lattice properties are uniform.

Experiments are carried out for different values of the induction and of the external force. After a stationary state is obtained (characterized by a steady average velocity), a snapshot of the moving lattice is recorded, on which a Delaunay triangulation is performed. Positive and negative disclinations (vortices with coordination 5 and 7), either free or forming dislocations by pairs[4] are counted. Samples typically enclose 7000 vortices and 4×10^4 pins.

III. RESULTS AND DISCUSSION

As shown in ref.[5], as the driving force decreases, the system evolves from a moving crystal to an amorphous phase. Contrasting with the results in [6, 7, 8], the high velocity phase does not show here smectic ordering, as evidenced from the direction pattern: this comes from the small ratio r_p/a_0 and from the fact that the tilted pinning potential shows here a moderate anisotropy on the scale of a_0 . There is no attractive interaction between the vortices, which would allow for a transition between a liquid and a gas. However, considering the comparable densities of the crystal and the less ordered phase, as well as the strong interactions between the vortices in the amorphous phase, it must obviously be called a 'liquid phase'. As evidenced in Fig.1 and 2 and the inspection of the average hexatic parameter, $j < j_c > = j < j > - j < j >_c = 1/c \sin^2 \theta$, where c is the coordination number for vortex and θ is the angle of the bond between neighboring vortices and, some residual orientational correlation is retained for $j < j_c$ ($j < j_c > < 0.1$), which justifies to call the low j phase an 'hexatic liquid'[7].

I now examine in more detail the transition between the crystal and the liquid. For all systems, the concentration of defects exhibits a clear onset upon decreasing the driving force, similar to the one reported in [1]. However, depending on the magnetic pressure, a discontinuous or gradual rise of this concentration is observed. This may be seen in Figs. 1 and 2 obtained for two different magnetic inductions, which clearly exhibit respectively a gradual and a step increase of the number of defects. In order to quantify this observation, the defects concentration was fitted with an exponential, $n_d / n_0 = 1 - \exp[-(j_c - j)]$ ($j < j_c$), yielding the onset, j_c , and a width for the transition to the liquid phase, Δj . In the framework of the theory for the equivalent 'shaking temperature'[1], this temperature is proportional to the magnitude of the pinning potential and to the inverse of the average velocity of the lattice. As a consequence, the representation of the data with the coordinates $(1 - j) = j$ and B appears as a way to obtain a phase diagram equivalent to the temperature-density representation for the thermodynamics. The onset for the defects concentration (j_c), as well as the location where it saturates ($j_c + \Delta j$), are plotted in this representation in Fig.3. Clearly, there is a range of magnetic induction for which a regime, in-

termEDIATE between the moving crystal and the hexatic liquid, can be found. The existence of such a regime was already pointed out in [5].

In order to characterize the continuous transition, let us examine some autocorrelation functions which are classical tools for the study of solids and liquids. The average hexatic order parameter does not provide an accurate characterization of the intermediate regime: as may be seen in Fig. 1, following a sharp drop at $j = j_c$, there is no significant change at lower j where the density of defects however still exhibits significant variations. The spatial correlations of the hexatic parameter carry more useful information [4]. The correlator $\langle \delta(\mathbf{r}) \delta(\mathbf{r}') \rangle_r$ for the data in Fig.1 is shown in Fig.4. Besides the existence of a non zero background related to the non zero averaged value $j < j_c > = j_c$, it reveals some additional short range correlations of the orientational order, which extends to a larger range as the system is closer to j_c . The oscillations for small r reflect the existence of a crystalline order within this range: they are associated with the fluctuations of the density autocorrelation function which come with the translational symmetry breaking of the crystal order. This is confirmed by the examination of the growth of the displacement field (actually a positional correlation function): $\langle u^2(\mathbf{r} = n a_0) \rangle = \langle u^2(n [r_j - r_i]) \rangle_i$ where j denotes one of the nearest neighbors of vortex i in a Delaunay triangulation and u is the displacement field from the periodic arrangement. As may be seen in Fig. 5, there is an exponential decay of the positional correlations, with a diverging correlation length as one approaches j_c from below (i.e. from larger temperatures). Following ref. [4], one may then call this regime an 'hexatic liquid crystal'. It is possible to track the positional correlation length, $\langle j \rangle$, in Fig.5 as one approaches j_c . The result is displayed in Fig.7 showing a divergence as $\langle j \rangle = j_c (1 - j/j_c)^{-1}$, with the bare correlation length $\approx 0.15 a_0$. Recalling the Lindemann melting criterion, $\langle u^2 \rangle = c_L^2 a_0^2$ and the exponential increase of the displacement field, $\langle u^2 \rangle = \langle u^2(1) \rangle (1 - \exp(-r/a_0))$, one may write an equivalent melting criterion for the present case as $a_0 = \ln(1 - c_L^2 a_0^2 / \langle u^2(1) \rangle)$. The result obtained using $c_L = 0.2$ and $\langle u^2(1) \rangle = 0.14$, $a_0 = 0.3$, is displayed in Fig.1 and 7. Although this quantitative result should be considered with caution, due to the uncertainty on the effective Lindemann number, this confirms that the solid has not melted in the conventional way below the threshold value j_c . As a further evidence for a spatially inhomogeneous situation, I plot in Fig.8 the local hexatic order parameter, which clearly shows intricate 'ordered' and 'disordered' phases.

The observation that the transition is continuous and involves a proliferation of defects appeals for a comparison with a Kosterlitz-Thouless transition. Unlike what is expected for such a transition, dislocations do not dissociate here at j_c to form an homogeneous 'plasma'. Rather, they tend to form chains of alternating positive (five-coordinated) and negative (seven-coordinated) disclinations

tions. As a result, unbounded dislocations and disclinations remain marginal (Fig. 6). In order to explain the formation of these chains, the examination of the early creation of defects in a driven crystal may be useful. Snapshots of the earlier defects detected in a sample driven in the intermediate region in Fig.1 are displayed in Fig.9. After a dislocation pair with opposite Burger vectors has been created by the pinning of one vortex (a), it is seen that the dislocations quickly arrange to form rings of diameter $2 a_0$ (c) and then larger loops (d). Remarkably, the composite defects reflect the external force anisotropy as soon as the dislocations dissociate (b): this results from the plastic mechanism at work to create these defects. This is also a direct evidence that the correlations in the pseudo random force cannot be neglected in their formation. The relation between these initial stages and the formation of chains is not completely clear. A possible mechanism is the stretching

of elementary loops as in Fig.9d, as the vortices making disclinations appear to become more easily pinned than the regular ones. This would make the long-range 'random force' correlations a key ingredient in the chain formation again. Equivalent rates for the growth and the annihilation of the chains would then account for the existence of a stationary regime intermediate between the crystal and the liquid.

In conclusion, it is found that a vortex lattice driven on dense quasi-point pins shows a continuous transition between the crystal and the liquid at intermediate induction, while first order otherwise. The binding of the disclinations in chains is proposed as a key mechanism to account for the existence of the continuous transition.

Simulations have been performed on the cluster of the Centre de Ressources Informatiques de l'Université Paris-Sud (CRI).

[1] A.E. Koshelev and V.M. Vinokur, *Phys. Rev. Lett.* 73, 3580 (1994).
[2] L. Balents, M.C. Marchetti, and L. Radzhovskiy, *Phys. Rev. B* 57, 7705 (1998).
[3] P. Le Doussal and T. Giamarchi, *Phys. Rev. B* 57, 11356 (1998).
[4] D.R. Nelson and B.I. Halperin, *Phys. Rev. B* 19, 2457 (1979).
[5] L. Fruchter, *Eur. Phys. J. B* 25, 313 (2002).
[6] K. Moon, R.T. Scalettar, G.T. Zimanyi, *Phys. Rev. Lett.* 77, 2778 (1996).
[7] R. Seungoh, M. Hellervist, S.D. Oniach, A. Kapitulnik, D. Stroud, *Phys. Rev. Lett.* 77, 5114 (1996).
[8] C.J. Olson, C. Reichhardt, F. Nori, *Phys. Rev. Lett.* 81, 3757 (1998).

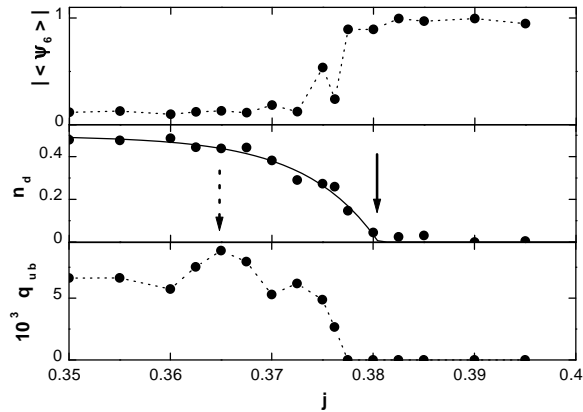


FIG .1: $B = 3950$ O e. From top to bottom : Hexatic parameter, concentration of defects, concentration of free disclinations. The line is the t described in the text; the full line arrow indicates the onset for the defects creation, as obtained from this t ; the dotted one is the melting point as obtained in Fig.7.

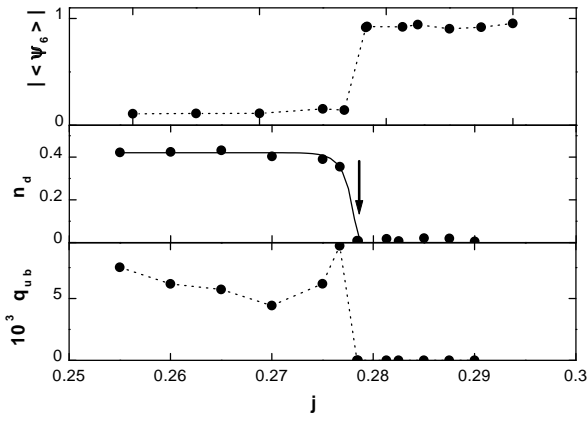


FIG .2: $B = 10^4$ O e.

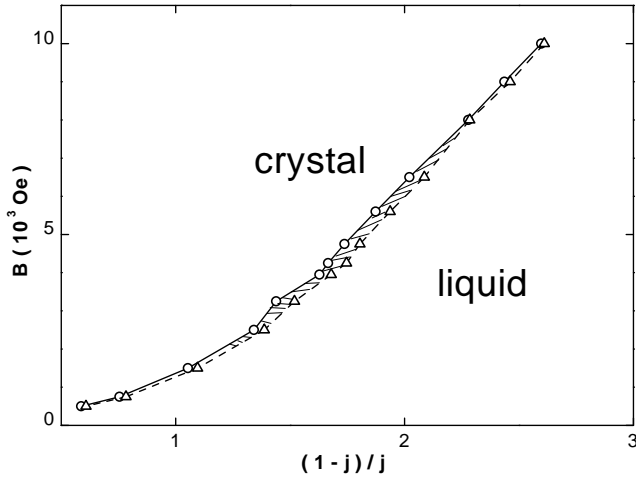


FIG. 3: Dynamical phase diagram of the driven lattice. Circles: $j = j_0$, triangles: $j = j_0$.

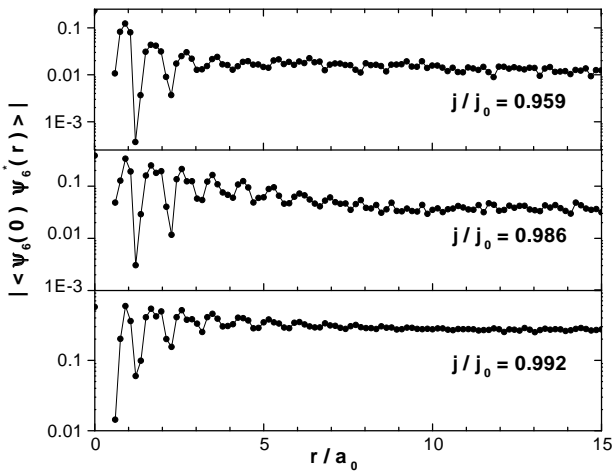


FIG. 4: The correlation function for the hexatic parameter.
($B = 3950$ Oe)

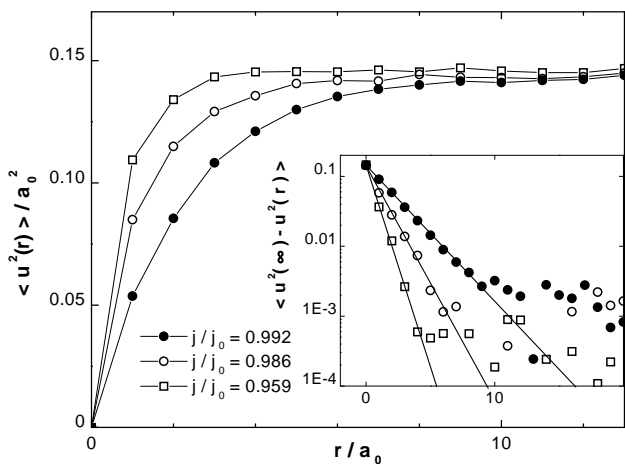


FIG. 5: The correlation function for the displacement field.
($B = 3950$ Oe)

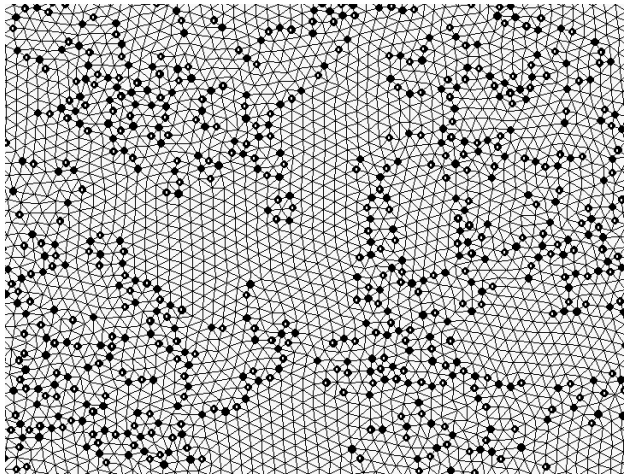


FIG .6: Positive - ve-coordinated (white centered) and negative - seven-coordinated disclinations in a sample driven along the vertical axis . ($B = 3950$ O e, $j = 0.375$)

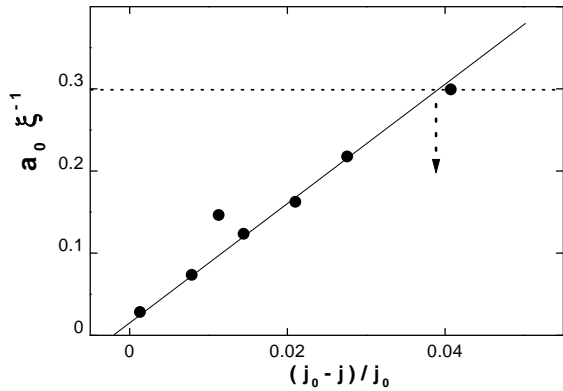


FIG .7: $B = 3950$ O e. Correlation length for the positional order, as obtained from the data in Fig.5. The full line is a linear t . The dotted line represents $\langle u^2 \rangle = c_L^2 a_0$ with $c_L = 0.2$. The melting point, as indicated by the dotted arrow , is shown in Fig.1 also.

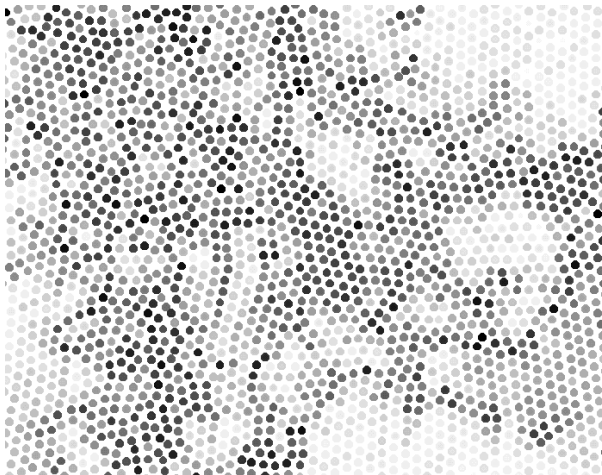


FIG . 8: $B = 3950 \text{ Oe}$, $j = 0.376$. A representation of the local hexatic order parameter. Darker vortices are the ones with the lower magnitude of the order parameter.

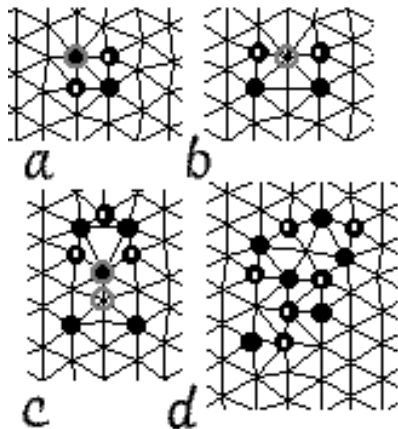


FIG . 9: Early steps for the creation of defects ($B = 3950 \text{ Oe}$, $j = 0.375$; gray circles indicate trapped vortices). Configurations a) and b) are obtained consecutively as the result of the trapping of one vortex. Configurations c) and d) are later steps. Vortices are driven to the top of the figure.